11-2010

Non-Certainty-Equivalent Adaptive Control of a Nonlinear Aeroelastic System

Keum W. Lee
Kwandong University, Gangwon, kwlee@kwandong.ac.kr

Sahjendra N. Singh
University of Nevada, Las Vegas, sajendra.singh@unlv.edu

jet INTL JOURNAL OF ELECTRONICS AND TELECOMMUNICATIONS, 2010, VOL. 56, NO. 4, PP. 463–471
Manuscript received April 16, 2010; revised August 2010. DOI: 10.2478/v10177-010-0063-7

Non-Certainty-Equivalent Adaptive Control of a Nonlinear Aeroelastic System

Keum W. Lee and Sahjendra N. Singh

***Abstract*—The development of a non-certainty-equivalent adaptive control system for the control of a nonlinear aeroelastic system is the subject of this paper. The prototypical aeroelastic wing section considered here includes structural nonlinearity and a single control surface for the purpose of control. Its dynamical model has two-degree-of-freedom and describes the plunge and pitch motion. It is assumed that the model parameters (except the sign of one of the control input coefficients) are not known. The uncontrolled aeroelastic model exhibits limit cycle oscillation beyond a critical free-stream velocity. Based on the attractive manifold, and the immersion and invariance methodologies, a non-certainty-equivalent adaptive state variable feedback control law for the trajectory tracking of the pitch angle is derived. Using the Lyapunov analysis, asymptotic convergence of the state variables to the origin is established. It is shown that the trajectory of the system converges to a manifold. The special feature of the designed control system is that the closed-loop system asymptotically recovers the performance of a deterministic controller. This cannot happen if certainty-equivalent adaptive controllers are used. Simulation results are presented which show that the control system suppresses the oscillatory responses of the system in the presence of large parameter uncertainties.**

***Keywords*—Aeroelastic wing, adaptive flutter control, nonlinear system, immersion and invariance method, uncertain system.**

I. Introduction

AEROELASTIC systems have rich dynamics and can exhibit a variety of phenomena including instability, limit cycle, and even chaotic vibration [1], [2]. In the past, researchers have made many important contributions related to aeroelastic behavior, stability and control of linear and nonlinear aeroelastic systems. Readers may refer to [3] which provides a historical perspective on analysis and control of aeroelastic systems. For aeroelastic models with parametric uncertainties, stability analysis using μ method has been attempted [4]. For a benchmark active control technology (BACT) wind-tunnel model constructed at the NASA Langley Research Center, control algorithms for flutter suppression have been developed [5], [6]. Based on classical, minmax, and passification methods, robust control systems for flutter control have been proposed [7], [8]. Control systems using gain scheduling method have been also attempted [9]. Neural and adaptive controllers for a transonic wind-tunnel model have been proposed [10], [11].

A two-degree-of-freedom aeroelastic model has been developed and tests have been performed in a wind tunnel to examine the effect of nonlinear structural stiffness. For this model, control systems have been designed using linear control theory and feedback linearization technique [12]–[14]. Furthermore for the model with parametric uncertainties, a variety of robust, and direct and indirect adaptive control systems have been developed [15]–[19]. The design of these adaptive laws are based on the certainty-equivalence principle. In certainty-equivalent adaptive (CEA) systems, the estimated parameters generated in the adaptive loop are directly used for synthesis without any modification [20], [21].

A new class of adaptive control systems based on the immersion and invariance (I&I) theory has been designed for nonlinear systems [22]–[24]. This method provides non-certainty-equivalent adaptive (NCEA) control systems. Unlike the CEA systems, the estimated parameters of the NCEA system includes not only the estimates generated by the adaptive dynamic subsystem but also include nonlinear functions. The additional nonlinear terms in the estimated parameter vector provide improved performance of the controller. For the application of the method of [22]–[24], one needs to satisfy certain integrability conditions, which are not easy. In order to avoid restriction posed by the integrability conditions of the I&I method, a design technique (termed attractive manifold method) for the derivation of NCEA law using filtered signals has been developed [25], [26]. The approach essentially sets up the design problem based on the filtered signals and uses parameter estimates combined with nonlinear functions similar to the I&I method. As such the attractive manifold method shares some features inherent to the I&I methodology. Using this approach, authors have developed NCEA laws for the attitude control of a rigid body and robotic systems [25], [26]. Based on the immersion and invariance approach of [22]–[24], NCEA control systems for the control of an aeroelastic system and a satellite using solar radiation pressure have been also developed [27], [28].

The NCEA law designed for the aeroelastic system of [27] based on the I&I method, uses plunge acceleration and state variables for feedback. Furthermore, the analytical computation in [27] is involved. As such it is of interest to develop new NCEA control laws for aeroelastic systems which are relatively simple from the viewpoint of analytical computation and use only state vector for feedback.

In this paper, the design of a non-certainty-equivalent adaptive control system for the control of an aeroelastic system is considered. This aeroelastic model has two-degree-of freedom and governs the nonlinear plunge and pitch motion [12], [13] of the wing section. This type of model has been traditionally used for the theoretical as well as experimental analysis of

Keum W. Lee is with the Division of Electronic information and Communication Eng., Gangwon 210-701, S. Korea.

Sahjendra N. Singh is with Department of Electrical and Computer Engineering, University of Nevada, Las Vegas, NV. 89154-4026 (e-mail: sahaj@egr.unlv.edu)

two-dimensional (plunge and pitch) aeroelastic behavior. The model has pitch polynomial type structural nonlinearities and uses a single control surface for the purpose of control. It is assumed that all the system parameters, except the sign of a single control input coefficient, are not known. The aeroelastic model has quasi-steady linear aerodynamic aerodynamics; however, it is noted that one can extend this approach to the case of nonlinear aerodynamics as well. This aeroelastic model exhibits limit cycle oscillations when the free-stream velocity exceeds a critical value. Based on the attractive manifold, and the immersion and invariance methodologies of [24]–[26], a non-certainty-equivalent adaptive control system for the pitch angle trajectory control is derived. Unlike the NCEA law designed in [27] for this model, here measurement of plunge acceleration is not needed, and for synthesis only the state variables are used. The NCEA control system has a modular structure and consists of a parameter estimator and a control module. It is shown that in the closed-loop system, the pitch angle trajectory converges to the reference trajectory, and oscillations in the state variables are suppressed. Furthermore, it is seen that in the closed-loop system, trajectories asymptotically converge to a manifold. Interestingly, once the trajectory converges to this manifold, the control system recovers the performance of a deterministic system. This special feature cannot be seen in CEA control systems. Simulation results for the control of oscillatory responses of the aeroelastic system for various flow velocities and elastic axis locations using the NCEA law are presented. It is seen that the controller accomplishes regulation of the state vector to the origin despite large parameter uncertainties.

The organization of the paper is as follows. Section 2 presents the aeroelastic model. A control module is designed in Section 3. This is followed by the design of a parameter identifier in Section 4. Finally, Section 5 presents the simulation results.

II. Aeroelastic Model and Control Problem

Fig. 1 shows the aeroelastic model. A laboratory model of this has been developed at the Texas A&M University for performing experiments. This model has two-degree-of-freedom, and its plunge and pitch motion is described by a system of dimension four.

The governing equations of motion are provided in [13] which are given by

$$\begin{bmatrix} m_t & m_w x_\alpha b \\ m_w x_\alpha b & I_\alpha \end{bmatrix} \begin{bmatrix} \ddot{h} \\ \ddot{\alpha} \end{bmatrix} + \begin{bmatrix} c_h & 0 \\ 0 & c_\alpha \end{bmatrix} \begin{bmatrix} \dot{h} \\ \dot{\alpha} \end{bmatrix} + \begin{bmatrix} k_{h0} & 0 \\ 0 & k_\alpha(\alpha) \end{bmatrix} \begin{bmatrix} h \\ \alpha \end{bmatrix} = \begin{bmatrix} -L \\ M \end{bmatrix} \tag{1}$$

where h is the plunge displacement and α is the pitch angle. In equation (1), m_w is the mass of the wing; m_t is the total mass; b is the semichord of the wing; I_α is the moment of inertia; x_α is the nondimensionalized distance of the center of mass from the elastic axis; c_α and c_h are the pitch and plunge damping coefficients, respectively; and M and L are the aerodynamic moment and lift. It is assumed that the quasi-steady aerodynamic force and moment are of the form

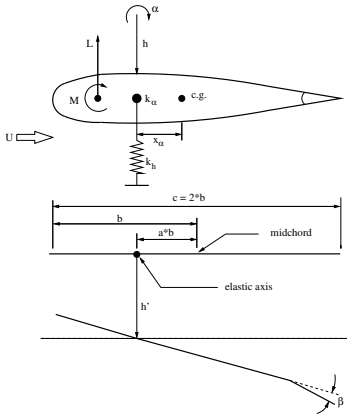

Fig. 1. Aeroelastic model.

$$\begin{aligned} L &= \rho U^2 b c_{l_\alpha} s_p \left[\alpha + \frac{\dot{h}}{U} + \left(\frac{1}{2} - a\right) b \frac{\dot{\alpha}}{U}\right] \\ &\quad + \rho U^2 b c_{l_{\beta_f}} s_p \beta_f \\ M &= \rho U^2 b^2 c_{m_\alpha} s_p \left[\alpha + \frac{\dot{h}}{U}\left(\frac{1}{2} - a\right) b \frac{\dot{\alpha}}{U}\right] \\ &\quad + \rho U^2 b^2 c_{m_{\beta_f}} s_p \beta_f \end{aligned} \tag{2}$$

where a is the nondimensionalized distance from the midchord to the elastic axis, s_p is the span, c_{l_α} and c_{m_α} are the lift and moment coefficients per angle of attack, and $c_{l_{\beta_f}}$ and $c_{m_{\beta_f}}$ are lift and moment coefficients per control surface deflection β_f. The nonlinear function $k_\alpha(\alpha)$ has a polynomial form of degree four and is given by

$$k_\alpha(\alpha) = k_{\alpha_0} + k_{\alpha_1}\alpha + k_{\alpha_2}\alpha^2 + k_{\alpha_3}\alpha^3 + k_{\alpha_4}\alpha^4$$

Of course the design method is applicable to any linearly parameterized nonlinear function $k_\alpha(\alpha)$.

Define the state vector as $x = (x_1, ..., x_4)^T = (\alpha, h, \dot{\alpha}, \dot{h})^T \in R^4$. Then the state space representation of equation (1) can be expressed as

$$\begin{aligned} \dot{x} &= \begin{bmatrix} 0_{2\times 2} & I_{2\times 2} \\ M_s & M_d \end{bmatrix} x + \begin{bmatrix} 0_{2\times 2} \\ g_0 \end{bmatrix} k_{n_\alpha} + \begin{bmatrix} 0_{2\times 1} \\ b_0 \end{bmatrix} \beta_f \\ &\doteq f(x) + B_0 \beta_f \end{aligned} \tag{3}$$

where $f(x)$ and B_0 are defined in equation (3), $\alpha k_\alpha = \alpha k_{\alpha_0} + k_{n_\alpha}$, $k_{n_\alpha} = \alpha(k_{\alpha_1}\alpha + k_{\alpha_2}\alpha^2 + k_{\alpha_3}\alpha^3 + k_{\alpha_4}\alpha^4)$, k_{ij} are constants, $g_0 = (g_{0i})$ is 2×1 constant vector, $b_0 = (b_{01}, b_{02})^T$ (T denotes transposition), 0 and I denote null and identity matrices of indicated dimensions, and the matrices $M_a = (M_s, M_d) \in R^{2\times 4}$, g_0 and b_0 are easily obtained from equation (1). For the derivation of the control law, following assumption is made.

***Assumption 1*:** It is assumed that elements of M_a, g_0, b_0, and k_{α_j} associated with the structural nonlinearity are not known, but the sign of b_{01} is known.

The open-loop aeroelastic model has stable as well as unstable behavior depending on the free-stream velocity. For

the model parameters given in the appendix and $a = -0.6547$, the loci of the eigenvalues of the matrix A, as a function of U, are shown in Fig. 2(a). We observe that for U less than the critical value $U^* = 16.6750$, the eigenvalues of A are stable, and as U exceeds the critical value, two branches of the loci cross into unstable region in the complex plane. Indeed U is a bifurcation parameter, and as the loci cross the imaginary axis, the supercritical Andronov-Hopf bifurcation takes place and periodic orbits are born. The size of the orbit increases with U. Figures 2(b)-(c) show the the closed orbits in the $(\alpha, \dot{\alpha}, U)$ and $(h, \dot{h}, U)$ space for a set of values of U exceeding the critical value U^*. The oscillatory waveforms of α and h as functions of time for $U = 20$ (m/s) are shown in Figs. 2(e)-(f) for initial state $x(0)$=($\alpha(0) = 0.1$ (deg), $h(0) = 0.0001$(m), $0, 0)^T$. We observe that after a short transient period, the model exhibits limit cycle oscillation (LCO). Of course it is important to suppress the undesirable oscillatory responses by application of control signal.

Let α be the controlled output variable. Suppose that α_r is a specified bounded and smooth reference pitch angle trajectory which asymptotically converges to zero. We are interested in the design of a non-certainty-equivalent adaptive system for the pitch angle trajectory tracking and regulation of the state vector to the origin in the state space. The choice of convergent reference trajectory is essential because here the interest is in suppression of the oscillatory responses of the aeroelastic model.

In the next sections, the control system is designed. It has a modular structure consisting of a control module and a parameter estimator. The design is based on the the attractive manifold and the I&I methodologies of [24]–[26].

III. Non-Certainty-Equivalent Adaptive Control Module

First the design of the control module for the trajectory control of α is considered. Using equation (3), the pitch acceleration can be expressed as

$$\ddot{\alpha} = f_3(x) + b_{01}u = \phi(x)^T\theta + b_{01}u \tag{4}$$

where $u = \beta_f$, $f_3(x) = \phi^T(x)\theta$ is the third component of $f(x)$, $\theta \in R^8$ is the vector of unknown parameters, and

$$\phi(x) = (\alpha, h, \dot{\alpha}, \dot{h}, \alpha^2, \alpha^3, \alpha^4, \alpha^5)^T \in R^8$$

.

For controller design, consider a function s which is a linear combination of the tracking error $\tilde{\alpha} = \alpha - \alpha_r$ and its derivative given by

$$s = \dot{\tilde{\alpha}} + \lambda\tilde{\alpha} \tag{5}$$

where $\lambda > 0$. In view of equation (5), we observe that if s is zero, then the tracking error tends to zero. As such it is sufficient to design a controller which forces s to zero.

The derivative of s along the solution of equation (4) is given by

$$\dot{s} = \phi^T(x)\theta + b_{01}u - \ddot{\alpha}_r + \lambda\dot{\tilde{\alpha}} \tag{6}$$

Adding and subtracting $k_1 s$, equation (6) can be written as

$$\dot{s} = b_{01}[\phi^T(x)\theta b_{01}^{-1} + b_{01}^{-1}(-\ddot{\alpha}_r + \lambda\dot{\tilde{\alpha}} + k_1 s) + u] - k_1 s \tag{7}$$

where $k_1 > 0$. Define a vector function $\psi(x,t) \in R^9$ of the form

$$\psi^T(x,t) = [\phi^T(x), -\ddot{\alpha}_r + \lambda\dot{\tilde{\alpha}} + k_1 s] \tag{8}$$

and a parameter vector $p \in R^9$ as

$$p = \begin{bmatrix} \theta b_{01}^{-1} \\ b_{01}^{-1} \end{bmatrix}$$

Here p is the vector of unknown parameters and the argument t of ψ denotes its dependence on α_r and its derivatives. Then equation (7) can be written in a compact form as

$$\dot{s} = b_{01}[\psi^T(x,t)p + u] - k_1 s \tag{9}$$

The adaptive control system of [27], designed using the immersion and invariance approach, requires state and plunge acceleration ($\ddot{h}$) feedback. Here in order to avoid acceleration measurement for synthesis, filtered signals are introduced following the attractive manifold design method of [25], [26]. The signals s, ψ and u are passed through first order filters to generate signals s_f, ψ_f and u_f, respectively. These filtered signals satisfy

$$\begin{aligned} \dot{s}_f &= -\mu s_f + s \\ \dot{\psi}_f &= -\mu\psi_f + \psi \\ \dot{u}_f &= -\mu u_f + u \end{aligned} \tag{10}$$

where $\mu > 0$.

Now instead of equation (9), a new equation involving signals s_f, ψ_f and u_f are obtained for the derivation of the control law. Note that equation (10) implies that $s = (D + \mu)s_f$, $\psi = (D + \mu)\psi_f$ and $u = (D + \mu)u_f$, where $D = (d/dt)$ denotes the derivative operator. Substituting for s, ψ and u in equation (9) and factoring $(D + \mu)$ gives

$$(D + \mu)[\dot{s}_f - b_{01}(\psi_f^T p + u_f) + k_1 s_f] = 0 \tag{11}$$

Solving the differential equation (11), one obtains

$$\dot{s}_f - b_{01}(\psi_f^T p + u_f) + k_1 s_f = e^{-\mu t} su(0) \tag{12}$$

where

$$su(0) = \dot{s}_f(0) - b_{01}(\psi_f^T(0)p + u_f(0)) + k_1 s_f(0) \tag{13}$$

Thus equation (12) implies that

$$\dot{s}_f = b_{01}(\psi_f^T p + u_f) - k_1 s_f + \epsilon(t) \tag{14}$$

where $\epsilon(t) = e^{-\mu t} su(0)$. The dynamics of s_f includes an exponentially decaying signal $\epsilon(t)$. Since this signal vanishes asymptotically, it is ignored in the sequel for simplicity. (Later a simple modification in the analysis will be indicated for establishing stability if $su(0)$ is not zero).

Of course, it is possible to set the initial conditions properly so that $\epsilon(t) = 0$. For verifying this, first note that $\dot{s}_f(0) = -\mu s_f(0) + s(0)$. Then it follows from equation (13) that $su(0) = 0$ if $\psi_f(0) = 0$, $u_f(0) = 0$, and $s_f(0) = s(0)/(\mu - k_1)$. Of course, one can choose $\psi_f(0)$ and $s_f(0)$ as indicated here, and it will be seen later that indeed $u_f(0)$ becomes zero if $\psi_f(0) = 0$.

Ignoring $\epsilon(t)$ in equation (14) gives

$$\dot{s}_f = b_{01}(\psi_f^T p + u_f) - k_1 s_f \tag{15}$$

For the derivation of the control law, equation (14) is important. The parameter vector p is not known. Let $\hat{p}+\beta(s_f,\psi_f)$ be an estimate of p, and let the parameter error be

$$z=\hat{p}+\beta(s_f,\psi_f)-p \tag{16}$$

where β is nonlinear function of the indicated arguments. Later the dependence of β on the variables s_f and ψ_f will be justified. It is pointed out that the inclusion of the nonlinear function β in the parameter vector estimate is the main advantage of the I&I approach. In certainty-equivalent adaptive laws, β is set to zero.

In view of equation (15), we select a control law of the form

$$u_f=-\psi_f^T(\hat{p}+\beta) \tag{17}$$

(Note that $u_f(0)=0$ if $\psi_f(0)=0$.) Substituting equation (17) in (15), gives

$$\begin{aligned}\dot{s}_f&=b_{01}\left(\psi_f^Tp-\psi_f^T(\hat{p}+\beta)\right)-k_1s_f\\&=-b_{01}\psi_f^Tz-k_1s_f\end{aligned} \tag{18}$$

For stability analysis, consider a Lyapunov function

$$V_1=\frac{s_f^2}{2} \tag{19}$$

Its derivative along the solution of equation (18) is

$$\begin{aligned}\dot{V}_1&=s_f[-b_{01}\psi_f^Tz-k_1s_f]\\&\le-k_1s_f^2+|s_f||\psi_f^Tz||b_{01}|\end{aligned} \tag{20}$$

Using Young's inequality [21], one has

$$|s_f||\psi_f^Tz||b_{01}|\le\frac{k_1}{2}s_f^2+\frac{b_{01}^2}{2k_1}(\psi_f^Tz)^2$$

which can be substituted in equation (20) to yield

$$\dot{V}_1\le-\frac{k_1}{2}s_f^2+\frac{b_{01}^2}{2k_1}(\psi_f^Tz)^2 \tag{21}$$

From equation (21), it follows that V_1 (and therefore z) will be bounded provided that ψ_f^Tz is bounded. In the next section, an adaptation law is derived such that z and ψ_f^Tz have desirable behavior.

IV. Parameter Estimator Design

For the derivation of the adaptation law, let us obtain the dynamics of the parameter error z. Differentiating z gives

$$\dot{z}=\dot{\hat{p}}+\frac{\partial\beta}{\partial s_f}\dot{s}_f+\frac{\partial\beta}{\partial\psi_f}\dot{\psi}_f \tag{22}$$

Substituting the derivatives of s_f and ψ_f from equations (18) and (10) yields

$$\dot{z}=\dot{\hat{p}}+\frac{\partial\beta}{\partial s_f}(-b_{01}\psi_f^Tz-k_1s_f)+\frac{\partial\beta}{\partial\psi_f}(-\mu\psi_f+\psi) \tag{23}$$

In view of equation (23), we select the update law of the form

$$\dot{\hat{p}}=\frac{\partial\beta}{\partial s_f}k_1s_f-\frac{\partial\beta}{\partial\psi_f}(-\mu\psi_f+\psi) \tag{24}$$

Substituting equation (24) in (23), gives

$$\dot{z}=-\frac{\partial\beta}{\partial s_f}b_{01}\psi_f^Tz \tag{25}$$

For the stability analysis, consider a Lyapunov function given by

$$V_2=\frac{1}{2}z^Tz \tag{26}$$

Using equation (25), its derivative can be written as

$$\dot{V}_2=-z^T\frac{\partial\beta}{\partial s_f}b_{01}\psi_f^Tz \tag{27}$$

For making $\dot{V}_2$ negative semidefinite, one chooses

$$\frac{\partial\beta}{\partial s_f}=(sgn(b_{01}))\gamma_1\psi_f \tag{28}$$

where $\gamma_1>0$ is the adaptation gain. This equation can be integrated to give

$$\beta=(sgn(b_{01}))\gamma_1\psi_fs_f \tag{29}$$

Substituting equation (28) in (27) gives

$$\dot{V}_2=-\gamma_1|b_{01}||\psi_f^Tz|^2\le0 \tag{30}$$

Since V_2 is positive definite and $\dot{V}_2$ is negative semidefinite, $z=0$ is globally uniformly stable and $z\in L_\infty[0,\infty)$ (the set of bounded functions). Furthermore integrating equation (30) gives

$$\int_0^\infty|b_{01}|(\psi_f^Tz)^2dt\le V_2(0)$$

which implies that $\psi_f^Tz\in L_2[0,\infty)$ (the set of square integrable functions).

In the definition of function s in equation (5), the state variables h and $\dot{h}$ do not appear. Thus even if α happens to be identically zero, the stability of the complete system will depend on the behavior of h. Therefore, examination of the zero dynamics of the system is essential. The zero dynamics represent the residual motion of the system when α and $\dot{\alpha}$ vanish. The chosen reference trajectory α_r converges to zero since α is to be regulated to zero. Therefore, in the following analysis, for simplicity, we assume that the reference trajectory $\alpha_r(t)$ is zero. By defining new variables $\eta_1=b_{02}\alpha-b_{01}h$ and $\eta_2=\dot{\eta}_1$, one can show that

$$\dot{\eta}=A_\eta\eta+g_\eta(\alpha,\dot{\alpha}) \tag{31}$$

where A_η is a 2×2 constant matrix, g_η is a nonlinear function of indicated arguments satisfying $g_\eta(0,0)=0$ and $\eta=(\eta_1,\eta_2)^T\in R^2$. Thus the zero dynamics are described by $\dot{\eta}=A\eta$.

The following assumption is made.

***Assumption 2*:** For the aeroelastic model, the flow velocity and the elastic axis location are such that the matrix A_η is Hurwitz (i.e. the origin of the zero dynamics is exponentially stable).

Now the stability of the closed-loop system including the estimator and the control module is analyzed. Consider a composite Lyapunov function

$$V=V_1+r_1V_2|b_{01}|,r_1>0 \tag{32}$$

Using equation (21) and (30), the derivative of V takes the form

$$\dot{V} \leq \left\{ -\frac{k_1}{2} s_f^2 + \frac{b_{01}^2}{2k_1} (\psi_f^T z)^2 \right\} - r_1 \cdot \gamma_1 |b_{01}| |\psi_f^T z|^2 \cdot |b_{01}| \quad (33)$$

We choose the weighting parameter satisfying $r_1 \geq \frac{1}{k_1 \gamma_1}$. Then it follows from equation (33) that

$$\dot{V} \leq -\frac{k_1}{2} s_f^2 - \frac{b_{01}^2}{2k_1} |\psi_f^T z|^2 \leq 0 \quad (34)$$

Noting that V is a positive definite function of s_f and z, and $\dot{V}_2 \leq 0$, one finds that $(s_f, z) \in L_\infty[0, \infty)$. Also integrating equation (34), one concludes that s_f and $\psi_f^T z$ are square integrable functions. According to the definition of the filtered signals, boundedness of s_f implies that s; and therefore, α and $\dot{\alpha}$ are bounded. Thus under Assumption 2, it follows that the state vector η is bounded, and therefore x is bounded. This implies that all signals in the closed-loop system and $\dot{s}_f$ are bounded. Then using the fact that $\phi_f^T z$ and s_f are bounded and square integrable, and that their derivatives are bounded, one has that s_f and $\phi_f^T z$ tend to zero. In view of equation (18), $\dot{s}_f$ is square integrable and moreover $\ddot{s}_f$ is bounded. From this one concludes that $\dot{s}_f$ tends to zero, which in view of equation (10) implies that s tends to zero. Of course α and $\dot{\alpha}$ tend to zero if s converges to zero. Finally one concludes convergence of x to the origin in view of Assumption 2.

Substituting β from equation (29) in (24) gives the update law

$$\dot{\hat{p}} = \gamma_1 (sgn(b_{01})) \psi_f s_f (k_1 + \mu) - \gamma_1 (sgn(b_{01})) s_f \psi \quad (35)$$

For synthesis, the input u is obtained from the filtered signal u_f using

$$u = (D + \mu) u_f = -(D + \mu)[\phi_f^T (\hat{p} + \beta)] \quad (36)$$

Note that $D = d/dt$. Using equation (36) and β from (29), and substituting for the derivatives of ψ_f, $\hat{p}$ and β, it is seen that the control input takes a simplified form given by

$$u = -\psi^T (\hat{p} + \beta) - \gamma_1 (sgn(b_{01})) \psi_f^T \psi_f [(k_1 - \mu) s_f + s] \quad (37)$$

Thus it is noted that the filtered signal u_f has been introduced here only for analysis and it is not needed for the implementation of the controller.

Now based on this derivation, the following theorem is stated.

***Theorem 1*:** Consider the closed-loop system equation (3) including the control and update laws (equations (37) and (35)). Suppose that Assumptions 1 and 2 are satisfied. Then in the closed-loop system, all the signals are bounded and $\tilde{\alpha}$, x, and $\psi^T z$ asymptotically converge to zero.

This derivation of control law has been done for the choice of proper initial conditions such that $\epsilon(t) = e^{-\mu t} s u(0) = 0$. Note that $\epsilon(t)$ satisfies $\dot{\epsilon}(t) = -\mu \epsilon(t)$. For $\epsilon(t) \neq 0$, $\dot{s}_f$ in equation (18) and $\dot{z}$ in equation (25) will have $\epsilon(t)$-dependent terms. To compensate for these functions, a modified Lyapunov function

$$V = \frac{s_f^2}{2} + \frac{r_1 z^T z}{2} + r_2 \epsilon^2$$

is chosen, where $r_2 > 0$. Such a modification for stability analysis for systems with additive decaying exponential signals is commonly used in adaptive literature [21]. Its derivative can be shown to be a negative definite function of s_f, $\psi_f^T z$ and $\epsilon(t)$ for sufficiently large positive values of r_1 and r_2, and therefore Theorem 1 remains valid.

The designed controller has an interesting feature. Let Ω be a manifold defined as

$$\Omega = \{(\psi_f, z) \in R^{18} : \psi_f^T z = 0\} \quad (38)$$

According to Theorem 1, one has that $\psi_f^T z$ converges to zero. As such the trajectory of the closed-loop system is eventually confined to the manifold Ω. Furthermore on this manifold, in view of equation (18), one has $\dot{s}_f = -k_1 s$. Of course, such a dynamics for s_f can be obtained by choosing a deterministic control law $u_f = -\psi_f^T p$ when the system parameters are known. Thus it follows that the NCEA law asymptotically recovers the performance of the deterministic controller. This has been possible due to inclusion of additional nonlinear function $\beta(s_f, \psi_f)$ in the parameter estimate.

V. Simulation Results

In this section, numerical results for the model given in Refs. [13] and [14] are obtained. The system parameters are given in the appendix. We assume that the initial conditions are $h(0) = 0.01$ (m), $\alpha(0) = 5$ (deg), $\dot{\alpha}(0) = \dot{h}(0) = 0$. The initial conditions of the filters are $\psi_f(0) = 0_{9\times 1}$ and $s_f(0) = 0$. For smooth regulation of the pitch angle, a fourth-order command generator of the form

$$(D^2 + 2\rho_1 \omega_1 D + \omega_1^2)(D^2 + 2\rho_2 \omega_2 D + \omega_2^2) \alpha_r(t) = 0$$

is used for generating reference trajectories for tracking. Its parameters are $\rho_1 = \rho_2 = 1$, and $\omega_1 = \omega_2 = 2$. The initial conditions are $\alpha_r(0) = \alpha(0)$ (deg) and $D^k \alpha_r(0) = 0$, $k = 1, ..., 3$. The controller gains are chosen to be $\lambda = 15$ and $k_1 = 15$. The adaptation parameter is $\gamma_1 = 0.2$, and filter parameter is $\mu = 20$. The initial estimate of the unknown parameter vector p is arbitrarily set as $\hat{p}(0) = 0$. The actual value of the parameter vector is given in the appendix. This is rather a worse choice of parameter estimates but is made to examine the robustness of the controller.

The poles of the linearized system for $U = 20m/s$ and $a = -0.6547$ are $1.1975 \pm 13.0787i$, $-3.3905 \pm 13.5807i$, and the zeros of the transfer function relating α and u are $-1.6279 \pm 17.5836i$. Thus the open-loop system is unstable and the linearized system has a minimum phase transfer function. The responses and the limit cycle for the open-loop system are shown in Fig. 2. Now the closed-loop responses for the model equation (1) with the control law equation (36) and adaptation law equation (35) are obtained.

***Case A*. Adaptive control:** $U = 20m/s$, $a = -0.6547$

First the closed-loop system for the choice of the free-stream velocity $U = 20m/s$, $a = -0.6547$ is simulated. The selected responses are shown Fig. 3 (a)-(h). We observe convergence of the tracking error and the state vector to zero in less than 5 seconds. The maximum tracking error is little over 3 (deg). The transients in the h-response is caused due to the complex

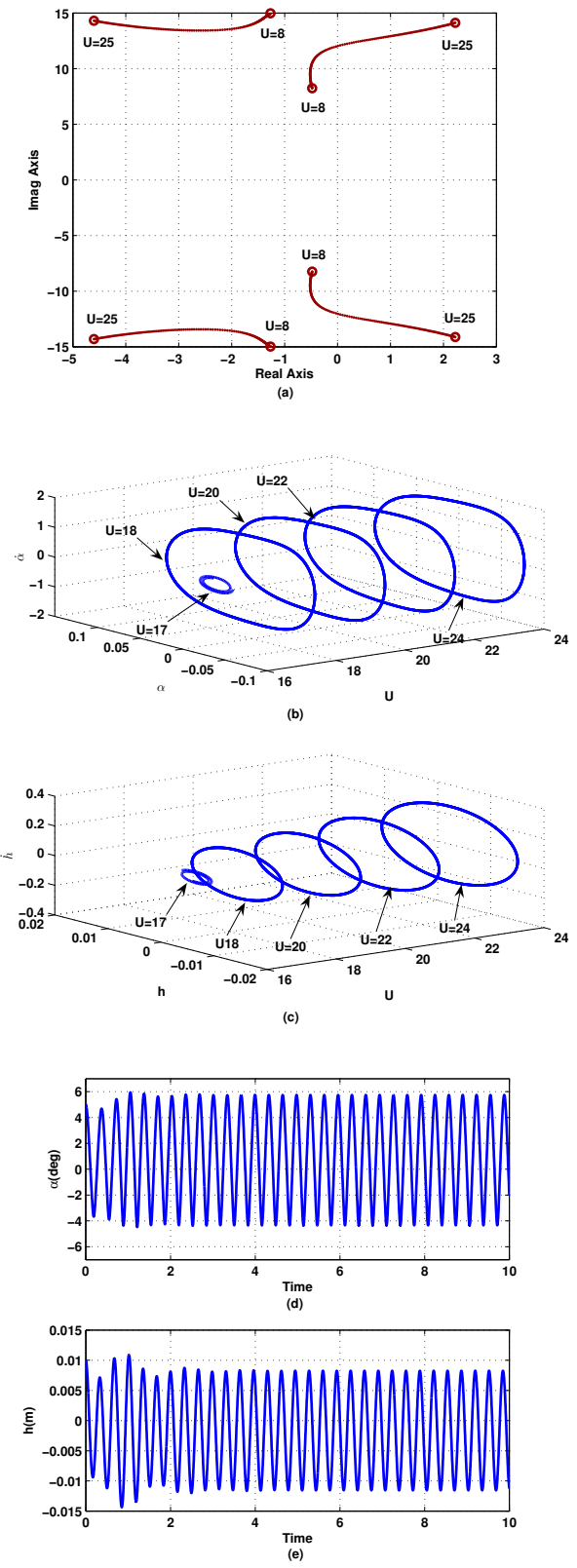

Fig. 2. Bifurcation of periodic orbits and LCO in the open-loop system $U = 20m/s$, $a = -0.6547$. (a) Loci plot for $U = [8, 25]$ (b) 3D plot $(\alpha, \dot{\alpha}, U)$ (c) 3D plot $(h, \dot{h}, U)$ (d) α for $U = 20m/s$, $a = -0.6547$ (e) h for $U = 20m/s$, $a = -0.6547$.

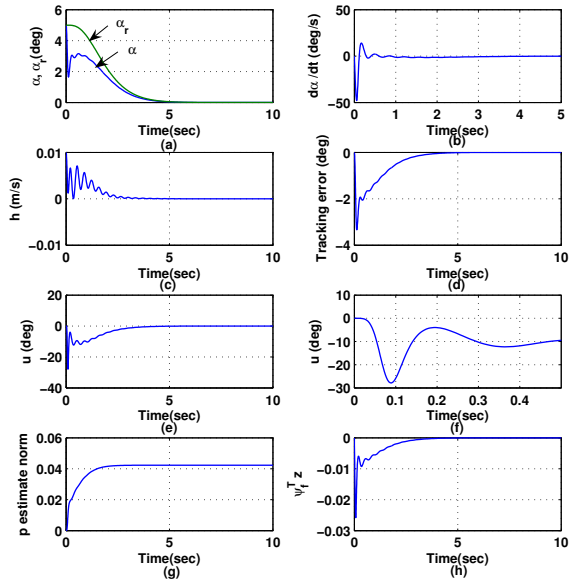

Fig. 3. Adaptive control: $U = 20m/s$, $a = -0.6547$. (a) Pitch angle α and reference pitch angle α_r (b) Pitch angle rate $\dot{\alpha}$ (c) Plunge displacement h (d) Tracking error of pitch angle α (e) Control input u (f) Control input u: initial period (g) Norm of $\hat{p}$ (h) $\psi_f^T z$.

zeros of the zero dynamics and coupling of the plunge-pitch dynamics. The parameter estimate vector $\hat{p} + \beta$ converges to some constant vector which differs from the actual value. This is not unusual, because convergence of parameters requires satisfaction of certain persistent excitation conditions. The plot of norm of $\hat{p}$ is shown in Fig. 3(g). As proven in Theorem 1, it is seen that $\psi_f^T z$ indeed converges to zero. As such the trajectories of the closed-loop system are eventually confined to the manifold M, and the adaptive controller recovers the performance of the deterministic system. The maximum value of flap deflection is 27.9 (deg).

Case B. **Adaptive control:** $U = 25m/s$, $a = -0.6547$

Now simulation is done to examine the sensitivity of the control system with respect to variation in the free-stream velocity. The chosen higher free-stream velocity is $U = 25m/s$, but parameters of the controller used for Case A are retained. The responses are shown in Fig. 4 (a)-(h). We again observe that the tracking error converges to zero, and the state vector tends to the origin in the state space. The response time remains less than 5 seconds. The maximum control surface deflection is 22.0 (deg). It is seen that the flap deflection is smaller compared to Case A. One would have expected this because the control effectiveness of the flap increases at higher free-stream velocity. The maximum tracking error is about 3.0 (deg).

Case C. **Adaptive control:** $U = 20m/s$, $a = -0.4$

In order to examine the robustness of the control system with respect to variations in a, simulation is performed for $U = 20m/s$ and a different value $a = -0.4$. The control gains, the filter parameter, and the adaptation gain of of case A are retained. Furthermore initial conditions have the same values

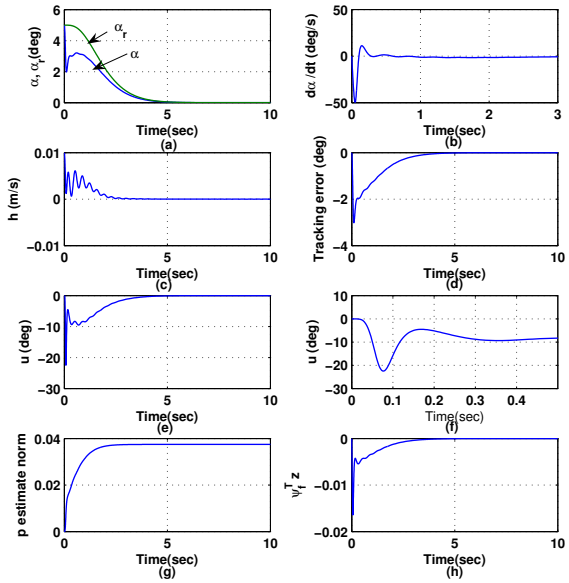

Fig. 4. Adaptive control: $U = 25m/s$, $a = -0.6547$. (a) Pitch angle α and reference pitch angle α_r (b) Pitch angle rate $\dot{\alpha}$ (c) Plunge displacement h (d) Tracking error of pitch angle α (e) Control input u (f) Control input u: initial period (g) Norm of $\hat{p}$ (h) $\psi_f^T z$.

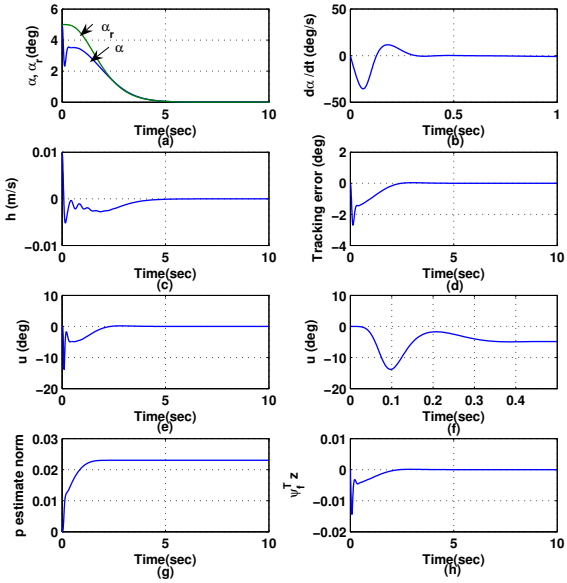

Fig. 5. Adaptive control: $U = 20m/s$, $a = -0.4$. (a) Pitch angle α and reference pitch angle α_r (b) Pitch angle rate $\dot{\alpha}$ (c) Plunge displacement h (d) Tracking error of pitch angle α (e) Control input u (f) Control input u: initial period (g) Norm of $\hat{p}$ (h) $\psi_f^T z$.

as of Case A. The selected responses are shown in Fig. 5 (a)-(h). We observe that oscillations in responses are suppressed within 5 seconds. The maximum control surface deflection is 2.7 (deg). It is seen that the control surface deflection for $a = -0.4$ is smaller compared to Case A and B with $a = -0.6547$. The maximum tracking error is 13.8 (deg), and $\psi_f^T z$ tends to zero.

***Case D*. Closed-loop control:** $U = 25m/s$**,** $a = -0.4$**,** $\alpha(0) = 10$ **(deg)**

Simulation is performed for $a = -0.4$ at a higher free-stream velocity of $U = 25m/s$. A larger perturbed initial condition for the pitch angle ($\alpha(0)$=10 (deg)) is assumed for this case. The controller parameters of case A are retained. The responses are shown in Fig. 6(a)-(h). We observe that the pitch angle tracking error converges to zero, and the plunge displacement and pitch angle trajectories are regulated to the origin. It is seen that due to larger perturbation in the initial state, larger control input magnitude (about 37.8 (deg)) compared to Case C is required in spite of the higher free-stream velocity. The tracking error is also larger in this case (little over 5 (deg)). But $\psi_f^T z$ converges to zero similar to other cases.

***Case E*. Closed-loop control for slow command:** $U = 20m/s$**,** $a = -0.6547$

Finally simulation results are presented for a slow command trajectory. The parameters ω_i of the command generator are $\omega_1 = \omega_2 = 1$, but all the remaining control system parameters of Case A are retained. The responses are shown in Fig. 7 (a)-(h). The plots show the convergence of the tracking error to zero and the state vector to the origin. But the response time is of the order of 9-10 seconds, which is almost double

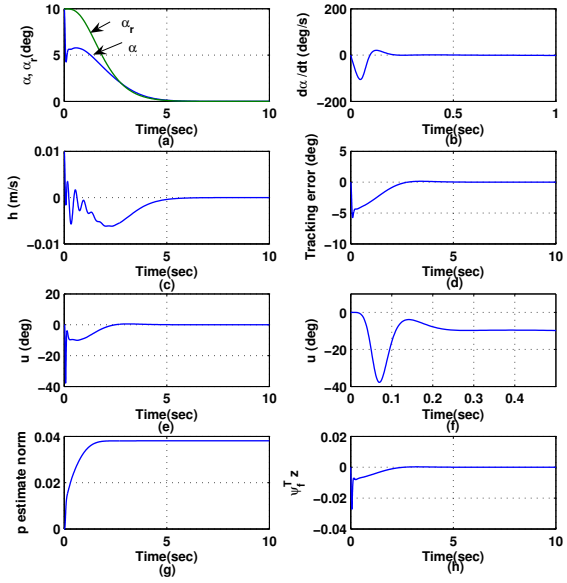

Fig. 6. Adaptive control: $U = 25m/s$, $a = -0.4$, $\alpha(0) = 10$ (deg). (a) Pitch angle α and reference pitch angle α_r (b) Pitch angle rate $\dot{\alpha}$ (c) Plunge displacement h (d) Tracking error of pitch angle α (e) Control input u (f) Control input u: initial period (g) Norm of $\hat{p}$ (h) $\psi_f^T z$.

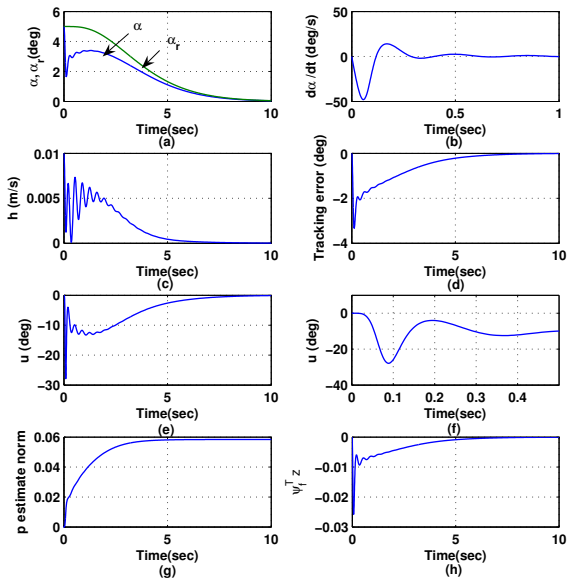

Fig. 7. Adaptive control with slow command: $U = 20m/s$, $a = -0.6547$, $\omega_1 = \omega_2 = 1$. (a) Pitch angle α and reference pitch angle α_r (b) Pitch angle rate $\dot{\alpha}$ (c) Plunge displacement h (d) Tracking error of pitch angle α (e) Control input u (f) Control input u: initial period (g) Norm of $\hat{p}$ (h) $\psi_f^T z$.

of the response time observed in Cases A to D. However maximum control input (27.9, deg) and tracking error (3.3, deg) magnitudes of Case A and Case E are of same order. This is attributed to the nonlinear time varying nature of the closed-loop adaptive system. We observe that the closed-loop trajectory converges to the manifold M ($\psi_f^T z$ tend to zero)

Extensive simulation has been performed for other values of the free-stream velocity and the parameter a. In each case, it has been observed that the NCEA law accomplishes control of the oscillatory motion of the aeroelastic system in spite of the uncertainties in the parameters.

To this end a comparison of the performance of the NCEA control system of this paper with the NCEA and the certainty-equivalent adaptive control systems derived in [27] will be appropriate. It is found that analytical derivation of control system in this paper is simpler compared to the derivation in [27]. We observe that for the chosen controller gains, the performance of this NCEA law with respect to convergence of tracking error and state vector is somewhat similar to the NCEA law of [27]. But here the control magnitude and tracking error are larger compared to those of [27]. Of course, unlike the controller synthesized here, the plunge acceleration, in addition to the state vector x, is used for controller implementation in [27]. The response time (about 5 seconds) of this closed-loop system is smaller compared to the response time (of the order of 9-10 seconds) of [27], because unlike [27] fast command trajectory is being tracked in Case (A)- (D) in this paper. But as seen in Case E here, for the same command trajectory, the response time of this NCEA system and the NCEA system of [27] are identical (9-10 seconds). It is also noted that similar to the NCEA law of [27], the control magnitude of this NCEA law for similar initial state perturbation (that is, Case (A)-(C) and (E)) is smaller compared to the certainty-equivalent adaptive system of [27]. Furthermore, the convergence of the trajectories to the manifold M defined in equation (38) is yet another advantage of the NCEA law over the CEA law. The CEA law in [27] does not have such kind of property because it does not have additional nonlinear function $\beta(x)$ in the parameter estimate.

VI. Conclusions

In this paper a new adaptive control system based on the attractive manifold, and the immersion and invariance methodologies was designed for the control of a nonlinear aeroelastic system. For the purpose of design, filtered signals were used. This design methodology gave a non-certainty-equivalent adaptive control law. The control system has a modular structure and includes a control module and a parameter identifier. Unlike the NCEA law published in literature, this controller was synthesized without acceleration feedback, and moreover the analytical computation has some simplicity. The stability analysis for the control module and the identifier was performed separately using two distinct Lyapunov functions. This allowed flexibility in adjusting the rate of convergence of parameter estimation error independently. Then using a composite Lyapunov function, it was shown that in the closed-loop system, all signals were bounded and the pitch angle trajectory tracking error and the plunge displacement asymptotically converged to zero. It was seen that asymptotically the trajectory converged to a manifold. Interestingly on this manifold, the system recovered the performance of a deterministic controller. Simulation results showed regulation of the pitch angle and plunge displacement to the origin in spite of large parameter uncertainties.

Appendix A
System Parameters and Estimation Parameters

1. System Parameters

$b = 0.135m$, $m_w = 2.049kg$, $c_h = 27.43Ns/m$, $c_\alpha = 0.036Ns$, $\rho = 1.225kg/m^3$, $c_{l_\alpha} = 6.28$, $c_{l\beta_f} = 3.358$, $c_{m_\alpha} = (0.5 + a)c_{l_\alpha}$, $c_{m_{\beta_f}} = -0.635$, $m_t = 12.387kg$, $I_\alpha = 0.0517 + m_w x_\alpha^2 b^2 kg \cdot m^2$, $x_\alpha = [0.0873 - (b + ab)]/b$, $k_\alpha = 2.82 * (1 - 22.1\alpha + 1315.5\alpha^2 - 8580\alpha^3 + 17289.7\alpha^4)N \cdot m/rad$, $k_{h0} = 2844.4N/m$

2. Poles and zeros of linearized model, and p

Case A.

Zeros : $-1.6279 \pm 17.5836i$

Poles : $1.1975 \pm 13.0787i$, $-3.3905 \pm 13.5807i$,

p : $1.0e + 004*$ [-0.0008, 0.0003, -0.0000, 0.0000, -0.0025, .1481, -0.9657, 1.9460, -0.0000]', where $p(9) = -0.0218$

Case B.

Zeros : $-1.6589 \pm 17.5807i$

Poles : $2.2236 \pm 14.1154i$, $-4.6026 \pm 14.3078i$

p : $1.0e + 004*$[-0.0005, 0.0002, 0.0000, 0.0000, -0.0016, 0.0948, -0.6181, 1.2454, -0.0000]', where $p(9) = -0.0139$

Case C.

Zeros : $-1.9561 \pm 15.3484i$

Poles : $-1.4539 \pm 14.9148i$, 3.0004, -3.5873

p : $1.0e+004$ *[-0.0001, -0.0000, -0.0000, 0.0000, -0.0019, 0.1137, .7414, 1.4940, -0.0000]', where $p(9) = -0.0159$

Case D.

Zeros : $-2.1566 \pm 15.3215i$

Poles : $6.6324, -7.3235, -1.4749 \pm 14.8472i$

p : $1.0e+003$ *[-0.0006, -0.0006, -0.0001, 0.0000, -0.0122, 0.7275, .7449, 9.5616, -0.0000]', where $p(9) = -0.0102$

Case E.

Zeros : $-1.6279 \pm 17.5836i$

Poles : $1.1975 \pm 13.0787i$, $-3.3905 \pm 13.5807i$

p : $1.0e+004$*[-0.0008, 0.0003, -0.0000, 0.0000, -0.0025, .1481, -0.9657, 1.9460, -0.0000]', where $p(9) = -0.0218$

REFERENCES

[1] Y. C. Fung, *An Introduction to the Theory of Aeroelasticity*. New York: Wiley, 1955, pp. 207–215.

[2] E. H. Dowell(Editor), *A Modern Course in Aeroelasticity*. MA: Kluwer Academic Publishers, 1995, ch. 1.

[3] V. Mukhopadhyay, "Historical perspective on analysis and control of aeroelastic responses," *Journal of Guidance, Control, and Dynamics*, vol. 26, no. 5, pp. 673–684, 2003.

[4] R. Lind and M. Brenner, *Robust Aeroservoelastic Stability Analysis*. Great Britain: Springer-Verlag, 1999.

[5] M. R. Waszak, "Robust multivariable flutter suppression for the benchmark active control technology wind- tunnel model," *Journal of Guidance, Control, and Dynamics*, vol. 24, no. 1, pp. 147–153, 2001.

[6] R. C. Scott, S. T. Hoadley, C. D. Wieseman, and M. H. Durham, "Benchmark active controls technology model aerodynamic data," *Journal of Guidance, Control and Dynamics*, vol. 23, no. 5, pp. 914–921, 2000.

[7] V. Mukhopadhyay, "Transonic flutter suppression control law design and wind-tunnel test results," *Journal of Guidance, Control and Dynamics*, vol. 23, no. 5, pp. 930–937, 2000.

[8] A. G. Kelkar and S. M. Joshi, "Passivity-based robust control with application to benchmark active controls technologywing," *Journal of Guidance, Control and Dynamics*, vol. 23, no. 5, pp. 938–947, 2000.

[9] J. M. Barker and G. J. Balas, "Comparing linear parameter- varying gain-scheduled control techniques for active flutter suppression," *Journal of Guidance, Control and Dynamics*, vol. 23, no. 5, pp. 948–955, 2000.

[10] D. M. Guillot and P. P. Friedmann, "Fundamental aeroservoelastic study combining unsteady computational fluid mechanics with adaptive control," *Journal of Guidance, Control and Dynamics*, vol. 23, no. 6, pp. 1117–1126, 2000.

[11] R. C. Scott and L. E. Pado, "Active control ofwind-tunnel model aeroelastic response using neural networks," *Journal of Guidance, Control and Dynamics*, vol. 23, no. 6, pp. 1100–1108, 2000.

[12] J. Ko, A. J. Kurdila, and T. W. Strganac, "Nonlinear control of a prototypical wing section with torsional nonlinearity," *Journal of Guidance, Control and Dynamics*, vol. 20, no. 6, pp. 1181–1189, 1997.

[13] J. Ko, T. W. Strganac, and A. J. Kurdila, "Stability and control of a structurally nonlinear aeroelastic system," *Journal of Guidance, Control, and Dynamics*, vol. 21, no. 5, pp. 718–725, 1998.

[14] J. J. Block and T. W. Strganac, "Applied active control for a nonlinear aeroelastic structure," *Journal of Guidance, Control, and Dynamics*, vol. 21, no. 6, pp. 838–845, 1998.

[15] K. W. Lee and S. N. Singh, "Global robust control of an aeroelastic system using output feedback," *Journal of Guidance, Control and Dynamics*, vol. 30, no. 1, pp. 271–275, 2007.

[16] W. Xing and S. N. Singh, "Adaptive output feedback control of a nonlinear aeroelastic structure," *Journal of Guidance, Control and Dynamics*, vol. 23, no. 6, pp. 1109–1116, 2000.

[17] J. Ko, T. W. Strganac, and A. J. Kurdila, "Adaptive feedback linearization for the control of a typical wing section with structural nonlinearity," *Nonlinear Dynamics*, vol. 18, no. 3, pp. 289–301, 1999.

[18] A. Behal, V. M. Rao, P. Marzocca, and M. Kamaludeen, "Adaptive control for a nonlinear wing section with multiple flaps," *Journal of Guidance, Control, and Dynamics*, vol. 29, no. 3, pp. 744–749, 2006.

[19] S. N. Singh and M. Brenner, "Modular adaptive control of a nonlinear aeroelastic system," *Journal of Guidance, Control, and Dynamics*, vol. 26, no. 3, pp. 443–451, 2003.

[20] K. S. Narendra and A. M. Annaswamy, *Stable Adaptive Systems*. NJ: Prentice Hall, 1989.

[21] M. Krstic, I. Kanellakopoulos, and P. Kokotovic, *Nonlinear and adaptive control design*. NY: John Wilely, 1995.

[22] A. Astolfi and R. Ortega, "Immersion and invariance : a new tool for stabilization and adaptive control of nonlinear systems," in *IEEE Transaction on Automatic Control*, vol. 48, no. 4, 2003, pp. 590–606.

[23] D. Karagiannis and A. Astolfi, "Nonlinear adaptive control of systems in feedback form : An alternative to adaptive backstepping," in *IFAC Symposium on Large Scale Systems : Theory and Applications*, 2004, pp. 71–76.

[24] A. Astolfi, D. Karagiannis, and R. Ortega, *Nonlinear and adaptive Control with applications*. London: Springer-Verlag, 2008.

[25] D. Seo and M. R. Akella, "High-performance spacecraft attitude-tracking control through attracting-manifold design," *Journal of Guidance, Control and Dynamics*, vol. 31, no. 4, pp. 884–891, 2008.

[26] D. Seo and M. Akella, "Non-certainty equivalent adaptive control for robot manipulator systems," *Systems & Control Letters*, vol. 58, pp. 304–308, 2009.

[27] K. W. Lee and S. N. Singh, "Immersion and invariance based adaptive control of a nonlinear aeroelastic system," *Journal of Guidance, Control, and Dynamics*, vol. 32, no. 4, pp. 1100–1110, 2009.

[28] ——, "Noncertainty-equivalent adaptive satellite attitude control using solar radiation pressure," *Proceedings of the Institution of Mechanical Engineers, Part G: Journal of Aerospace Engineering*, November 2009.